applied sciences

MDPI

Article

Partial Path Overlapping Mitigation: An Initial Stage for Joint Detection and Decoding in Multipath Channels Using the Sum–Product Algorithm

Anoush Mirbadin [1,*,†] and Abolfazl Zaraki [2,†]

[1] Department of Engineering, SELTA Digital Platforms Company, 29010 Cadeo, Italy
[2] School of Physics, Engineering and Computer Science (SPECS), University of Hertfordshire, Hatfield AL10 9AB, UK; a.zaraki@herts.ac.uk
* Correspondence: anoush.mirbadin@dplatforms.it
† These authors contributed equally to this work.

Abstract: This paper addresses the problem of mitigating unknown partial path overlaps in communication systems. This study demonstrates that by utilizing the front-end insight of communication systems along with the sum–product algorithm applied to factor graphs, it is possible not only to track these overlapping components accurately, but also to detect all multipath channel impairments simultaneously. The proposed methodology involves discretizing channel parameters, such as channel paths and attenuation coefficients, to ensure the most accurate computation of means of Gaussian observations. These parameters are modeled as Bernoulli random variables with priors set to 0.5. A notable aspect of the algorithm is its integration of the received signal power into the calculation of noise variance, which is critical for its performance. To further reduce the receiver complexity, a novel implementation strategy, based on provided pre-defined look up tables (LOTs) to the reciver, is introduced. The simulation results, covering both distributed and concentrated pilot scenarios, reveal that the algorithm performs almost equally under both conditions and surpasses the established upper bound in performance.

Keywords: joint; detection; decoding; multipath

Citation: Mirbadin, A.; Zaraki, A. Partial Path Overlapping Mitigation: An Initial Stage for Joint Detection and Decoding in Multipath Channels Using the Sum–Product Algorithm. *Appl. Sci.* **2024**, *14*, 9175. https://doi.org/10.3390/app14209175

Academic Editor: Christos Bouras

Received: 8 September 2024
Revised: 30 September 2024
Accepted: 8 October 2024
Published: 10 October 2024

1. Introduction

The initial approaches to reduce the effect of multipath impairment are broadly categorized into three main groups: diversity, multicarrier transmission, and their combinations. Diversity considerably reduces the probability of simultaneous fade on several replicas of the same information signal. Various diversity transmission techniques for fading environments have been extensively studied in [1–5]. In multicarrier modulation schemes like orthogonal frequency division multiplexing (OFDM), employing longer symbol durations effectively reduces the intersymbol interference (ISI), which can further be mitigated by utilizing cyclic prefixes. The effectiveness of OFDM and its application in combating ISI channels has been well investigated in [6]. Additionally, the combination of multicarrier modulation and diversity techniques has also been well addressed in the literature, e.g., [7,8].

Later, with the emergence of machine learning algorithms like expectation propagation (EP), new attempts to mitigate multipath phenomena in both time and frequency domains have been pursued [9,10]. However, EP has its drawbacks, such as numerical instabilities when performing distribution divisions [11]. As a result, our focus shifts toward the fundamental aspects of wireless communications. More recently, AI-assisted algorithms have been proposed to handle multipath channels [12]. In the first two studies, the channel parameters, such as the number of paths, path gains, and delays, are known as the receiver. To provide additional clarity, we will briefly outline the algorithm proposed in [9].

The receiver utilizes an equalizer based on EP. This equalizer employs the decoder feedback to execute the EP. Specifically, the posteriors generated by the decoder are mapped into Gaussian messages, with their means and variances dependent on channel impairments, such as channel taps. A similar methodology is applied in the frequency domain in [10]. In the last work, the number of channel taps is fixed, and it is assumed that the channel taps follow a Gaussian distribution with an exponential power profile, but the channel is not dense over a block of the received signal.

The main contribution of this paper is the design of a receiver that, instead of depending on the low-pass equivalent of the channels, is based on front-end communication systems. This design allows for the use of the sum–product algorithm (SPA) to simultaneously track all multipath channel parameters. In addition, a discretization and modeling technique for unknown channel parameters is introduced, where the parameters are represented as Bernoulli random variables. The SPA is then used to track the unknown parameters. Notably, the receiver does not require prior knowledge of the channel parameters, such as the number of paths or Gaussian channel taps. Moreover, extending this algorithm to the general multipath channels is straightforward.

This paper introduces a novel approach for performing joint partial path overlapping detection and channel decoding symbol by symbol in a dense partial path overlapping over a block of received symbols, utilizing the SPA on factor graphs. By focusing on front-end communication systems, we can track all unknown channel parameters through SPA on factor graphs. While this approach, i.e., the front-end receiver design using SPA, was initially proposed by the authors of this paper in [13], its advantages quickly gained the attention of researchers [14], where it has been named as discrete time models. In our study, we discretize channel parameters such as channel paths and attenuation coefficients, both in the channel low-pass equivalent (for illustrative purposes) and in the front-end strategy. These parameters are modeled as Bernoulli random variables with priors set to 0.5, denoted as path existence (PE) and attenuation existence (AE). Given a vector of observations, we factorize the joint posterior distribution of channel model parameters and codeword bits. SPA is then applied to the corresponding factor graph to compute the marginals of the desired random variables. The exact implementation of SPA results in a significant computational complexity. To reduce this considerably, we propose the use of pre-defined look-up tables (LOTs) at the receiver. The dimension of LOTs depends on the constellation symbols' dimensionality and the discretization levels of unknown channel parameters. Average signal power at the receiver determines the noise variance. However, when we compensate the reflected components in the means of Gaussain observations, we should remove the power of those components from the noise variance. This can also be accomplished through the provided LOTs for the receiver. We found that the constellation size dictates the quantity of estimated patterns of reflected rays, with only one occurring at each time epoch, similar to additive noise. Therefore, the receiver relies on making hard decisions based on the provided posteriors by the decoder to select the most suitable one among them. Performance evaluations are conducted through bit error rate (BER) curves in both distributed and concentrated pilots scenarios. As none of the channel parameters are known to the receiver, previous works, such as [9], were unable to effectively track these parameters. This limitation highlights the need to modify existing algorithms. For this reason, we introduce a relative solution as the upper bound of the system performance. The relative solution can also serve as a comparison benchmark in this context. Our simulation results prove that by increasing receiver' iterations, the BER curves differ from the relative solution considerably.

The paper is organized as follows: Section 2 introduces the discretization strategy for channel parameters, followed by the system model in Section 3. Section 4 discusses the corresponding factor graph and its SPA equations. Receiver implementations are detailed in Section 5, with performance analysis provided in Section 6. Finally, conclusions are drawn in Section 7.

2. Discretization Strategy

Consider the general model for a L-Path multipath channel (Equations (13.1)–(5) of [15], Equations (3.3)–(3.6) of [16])

$$h(\tau;t) = \sum_{i=0}^{L-1} \alpha_i(t) \exp(-j2\pi f_c \tau_i(t)) \exp\left(j2\pi \frac{v_i \cos\phi_i(t)}{c_0} f_c t\right) \delta(\tau - \tau_i(t)) \tag{1}$$

in which $\alpha_i(t)$ is the real-valued gain of i-th path, $\exp(-j2\pi f_c \tau_i(t))$ is the phase shift (often, these two terms are considered as one term, called the complex attenuation factor), f_c is the carrier frequency, $\tau_i(t)$ is the propagation delay of i-th path, v_i is the velocity associated with the i-th path, $\phi_i(t)$ is the angle of arrival of the wave (for the sake of simplicity, its value is assumed zero throughout this article), and c_0 is the speed of light. We consider that the channel remains constant during each symbol period. This implies that the channel can change symbol by symbol, i.e., L changes symbol by symbol. In this project, we model the path gain in (1) by the exponential function as $\alpha_i(t) = \exp(-\tau_i(t)a_i)$ in which a_i is the attenuation coefficient. It is assumed that τ_i is a Weibull random variable. The parameter of the Weibull distribution is adjusted such that its behavior closes a semi-exponential function. We assume that each $\tau_i(t)$ is smaller than the symbol duration T. This ensures partial paths overlapping across the successive symbol, and guarantees dense overlapping environment over a block of received symbols. At the receiver side, the following channel model is employed, i.e., all channel hypotheses are considered.

$$\begin{aligned} h(\tau;t) = \sum_{i=0}^{N-1} PE_i \exp\left(-iT_N \sum_{i'=1}^{N'} AE_{i'} i' a'_{N'}\right) \exp(-j2\pi f_c i T_N) \\ \times \exp\left(j2\pi \left(\sum_{i''=1}^{N''} \frac{VE_{i''} i'' V_{N''}}{c_0}\right) f_c t\right) \delta(\tau - iT_N) \end{aligned} \tag{2}$$

where $T_N = \frac{T}{N}$ is the delay resolution (T is the symbol duration), $a'_{N'} = \frac{1}{N'}$ is the attenuation resolution, and $V_{N''} = \frac{V_m}{N''}$ is the velocity resolution (in which V_m is the maximum possible velocity). PE, AE, and VE are Bernoulli random variables representing path, attenuation, and velocity existences, respectively. Their prior probabilities are set to 0.5. If N, N', and N'' go to infinity and we have exactly the knowledge of PE, AE, and VE, the error modeling goes to zero. It is important to highlight that the low-pass equivalent equations mentioned above primarily represent our discretization strategy. Our simulations are rooted in our front-end approach.

3. System Model

We start this research from the simplest case, i.e., baseband communications, to avoid missing all aspects of this research field. We consider a baseband communication system in which symbol duration is much smaller than the coherent time of the channel, and the Doppler effect is negligible. This assumption is unavoidable unless otherwise the baseband pulses will be broadened at the receiver due to the Doppler effect, and a high amount of interference corrupts the communication.

Consider a modern baseband communication system. The transmitter encodes data bits using a low-density parity-check (LDPC) encoder. Pilot symbols are inserted to enhance the performance of the receiver. This is followed by a binary pulse amplitude (B-PAM) modulator. The coded modulation symbols $\mathbf{c} = (\mathbf{c_0}, \mathbf{c_1}, ..., \mathbf{c_{K-1}})$ are pulsed-shaped using the root-raised cosine filter and then transmitted over an additive white Gaussian noise (AWGN) channel impaired by path overlapping.

4. Factor Graph

We consider a scenario where a maximum of N potential paths are considered during each time epoch, with $N-1$ of these paths susceptible to interference to the successive symbol. Additionally, we account for a maximum of N' discretization levels for attenuation coefficients. To illustrate, let us examine a channel model with $N = 2$. Here, at each time epoch, three paths emerge: the potential interfering path from the preceding symbol; the delayed version of the current symbol, encompassing segments of both the current and preceding symbols; and the direct line-of-sight (LOS) signal. Each of these paths undergoes processing via the receiver-matched filter to calculate the conditional Gaussian observation mean. To facilitate this, we conduct offline computations of the receiver-matched filter for all possible paths, constructing a LOT to simplify the message-passing algorithm. Consequently, four values, denoted as β_k, γ_k, ζ_k, and ψ_k, where k denotes the current time epoch, are acquired at the output of the receiver-matched filter. From the system model, the observation at time k can be determined by

$$r_k = \beta_k + \gamma_k + \zeta_k + \psi k + n_k, \ (k = 0, 1, ..., K-1) \tag{3}$$

The value r_k is acquired post receiver-matched filtering. The sequence $\{n_k\}$ comprises independent and identically distributed (i.i.d.) Gaussian noise components, denoted as $n_k \sim \mathcal{N}(n_k; 0, \sigma^2)$. ψ_k results from matched filtering of the LOS component. β_k arises from matched filtering a segment of the preceding symbol at time $k-1$, representing the delayed version of the symbol at time $k-1$. γ_k stems from matched filtering a segment of the preceding symbol at time k. ζ_k is obtained through matched filtering a segment of the current symbol at time epoch k. The computation of these signals, considering Equation (2), is summarized as

$$\psi_k = [c_k p(n)]_{n=0}^{NT_N} * p^*(-n)|_{n=NT_N} \tag{4}$$

in which $p(n)$ is the pulse shaping filter (here it is the root-raised cosine one). NT_N is the symbol duration.

$$\beta_k = \exp\Big(-lT_N l^{'} a^{'}(N^{'})\Big)[c_{k-1} p(n)]_{n=NT_N - lT_N}^{NT_N} * p^*(-n)|_{n=NT_N} \tag{5}$$

where l and $l^{'}$ are detected channel parameters for the non-LOS path at time epoch $k-1$.

$$\gamma_k = \exp\Big(-l^{''} T_N l^{'''} a^{'}(N^{'})\Big)[c_{k-1} p(n)]_{n=0}^{NT_N - l^{''} T_N} * p^*(-n)|_{n=NT_N} \tag{6}$$

$$\zeta_k = \exp\Big(-l^{''} T_N l^{'''} a^{'}(N^{'})\Big)[c_k p(n)]_{n=NT_N - l^{''} T_N}^{NT_N} * p^*(-n)|_{n=NT_N} \tag{7}$$

where $l^{''}$ and $l^{'''}$ are the detected channel parameters for the non-LOS path at time epoch k.

The receiver can be implemented through factorizing the joint posterior distribution of data bits and channel parameters, given the observation samples after the matched filter and applying the SPA to the corresponding factor graph.

$$\begin{aligned} p(\mathbf{b}, \mathbf{PE}, \mathbf{AE}|\mathbf{r}) \propto P(\mathbf{b})\mathbf{P}(\mathbf{PE})\mathbf{P}(\mathbf{AE})(\mathbf{r}|\mathbf{b}, \mathbf{PE}, \mathbf{AE}) \propto \\ \prod_{k=0}^{K-1} p\Big(r_k|c_k, c_{k-1}, \mathbf{PE^k}, \mathbf{PE^{k-1}}, \mathbf{AE^k}, \mathbf{AE^{k-1}}\Big) \prod_{k'=0}^{N-1} P(PE_{k'}^{k}) \prod_{k''=1}^{N^{'}} P(AE_{k''}^{k'}) \times \\ \prod_{k'''=1}^{N-1} P(PE_{k'''}^{k-1}) \prod_{k''''=1}^{N^{'}} P(AE_{k''''}^{k''}) T[\mathbf{c} = \mathbf{J_c}(\mathbf{b})] \end{aligned} \tag{8}$$

where $T[.]$ is the code indicator function that is equal to 1 if $\mathbf{c}$ is the codeword corresponding to $\mathbf{b}$, and to 0 otherwise. The detector estimates different patterns for paths at each time, conditioned on c_{k-1}, with only one occurring at any given moment. This concept will be

further explained in the following section. The corresponding factor graph is depicted in Figure 1. One can conclude by considering the mentioned example.

$$p\left(r_k|c_k, c_{k-1}, \mathbf{PE^k}, \mathbf{PE^{k-1}}, \mathbf{AE^k}, \mathbf{AE^{k-1}}\right) \propto \exp\left\{-\frac{(r_k-(\beta_k+\gamma_k+\zeta_k))^2}{2\sigma^2}\right\} \tag{9}$$

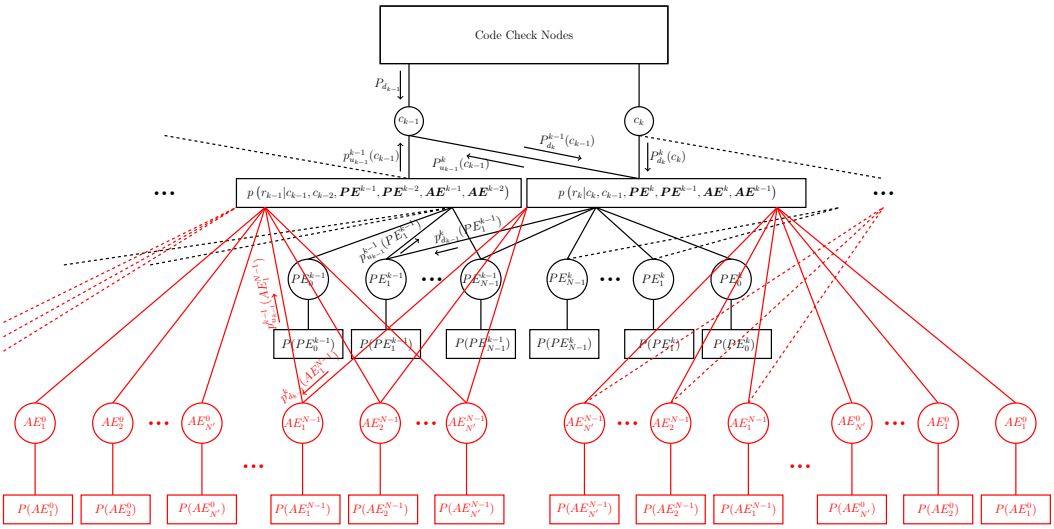

Figure 1. Factor graph representation of Equation (8). The receiver contains two detection algorithms, each corresponding to a specific unknown channel parameter. The variable node PE_i^k represents the i-th path existence at time k, while AE_i^k represents the i-th attenuation existence at the same time.

5. Implementation of the Receiver

The iterative receiver consists of two algorithms to detect PEs and AEs. This is followed by hard decisions on variable nodes. The detection is performed bit by bit. This detection process iterates, and after several iterations, LDPC decoding is executed. The entire process is reiterated a few times, followed by error rate computations at the receiver. During forward recursion, backward messages are not available. To compute the forward message at time epoch k, we assume that the decoder and detector have made their decisions on c_{k-1}, PE^{k-1}, and AE^{k-1} at time $k-1$, thus, they are known. Now, we compute the messages $p_{u_k}^k(c_k)$ and $p_{u_k}^{k+1}(\mathbf{PE^k})\mathbf{p_{u_k}^{k+1}}(\mathbf{AE^k})$. To achieve this, we calculate the following messages by applying the SPA on the corresponding factor graph.

$$p_{u_k}^k(c_k) = \prod_{n=0}^{N-1}\left(\sum_{PE_n^k} P(PE_n^k)\left(\sum_{AE_1^n} P(AE_1^n)\ldots\sum_{AE_{N''}^n} P(AE_{N''}^n)\right)\right) p\left(r_k|c_k, \mathbf{PE^k}, \mathbf{AE^k}\right) \tag{10}$$

$$\begin{aligned} p_{u_k}^{k+1}(PE_i^k) = &\sum_{c_k} P_{d_k}^k(c_k) \prod_{\substack{n=0\\ n\neq i}}^{N-1}\left(\sum_{PE_n^k} P(PE_n^k)\left(\sum_{AE_1^n} P(AE_1^n)\ldots\sum_{AE_{N''}^n} P(AE_{N''}^n)\right)\right)\times \\ &\left(\sum_{AE_1^i} P(AE_1^i)\ldots\sum_{AE_{N''}^i} P(AE_{N''}^i)\right) P(PE_n^k) p\left(r_k|c_k, \mathbf{PE^k}, \mathbf{AE^k}\right) \end{aligned} \tag{11}$$

$$p_{u_k}^{k+1}(AE_i^j) = \sum_{c_k} P_{d_k}^k(c_k) \prod_{\substack{n=1 \\ n\neq i}}^{N'} \left(\sum_{AE_n^j} P(AE_n^j) \right) \left(\sum_{PE_0^k} P(PE_0^k) \ldots \sum_{PE_{N-1}^k} P(PE_{N-1}^k) \right) \times \prod_{\substack{m=1 \\ m\neq j}}^{N'} \left(\sum_{AE_0^m} P(AE_0^m) \ldots \sum_{AE_{N'}^m} P(AE_{N'}^m) \right) P(AE_n^j) p\left(r_k | c_k, \mathbf{PE^k}, \mathbf{AE^k} \right) \tag{12}$$

Provided the fact that PE and AE are Bernoulli random variables and only one (PE, AE) pair occurs at every time epoch, the above equations form a Bahl–Cocke–Jelinek–Raviv (BCJR) algorithm. In this case, $p_{u_k}^{k+1}(PE_i^k)$ and $p_{u_k}^{k+1}(AE_i^j)$ are equal. This is followed by hard decisions to find the indices of (PE, AE) pair. A similar algorithm is employed to compute the backward messages. It should be noted that at every time epoch, we make hard decisions on $P_{d_{k-1}}$ and $P_{d_{k+1}}$ to determine the symbols c_{k-1} and c_{k+1}, respectively. Finally, the bit log-likelihood ratios (bitLLRs) are computed by

$$p_{u_k}(c_k) = p_{u_k}^{k+1}(c_k) p_{u_k}^k(c_k) \tag{13}$$

As implementing the SPA directly on such a factor graph is intricate, we propose a simplified implementation strategy to streamline the process and mitigate complexity issues. To realize Equations (10)–(12), we introduce four LOTs, each corresponding one-to-one with possible combinations of $c_{k-1}c_k$, as per Equations (4) to (7). These LOTs have dimensions $N \times N'$. Consequently, potential Gaussian observation means are computed prior to the receiver computations. Thus, the algorithm simplifies to:

- At every time epoch, the receiver performs matrix subtractions, r_k minus LOTs.
- Receiver finds the indices of the minimum matrices members of the detector's upward messages.

It is evident by considering the interference of the current symbol on many successive symbols only the number of LOTs increases. The main algorithm could still be implemented through matrix subtractions and finding the indices of the minimum value at every time.

To conclude this section, it is essential to highlight three key aspects of this research. Firstly, as per the aforementioned process, the receiver provides overlapping patterns at each time epoch, with the number of patterns equating to the constellation size. Only one pattern occurs at a time. We employ feedback from the decoder to select the pattern corresponding to the constellation symbol with the highest probability of occurrence. Secondly, the average signal power at the receiver determines the noise variance. However, when compensating for reflected components in the means of the Gaussian observations, it is crucial to remove the power of those components from the noise variance. We simplify this adjustment using the LOTs provided for the receiver. Finally, the Gaussian multiplication is employed, whenever it is needed, in the message passing algorithm.

6. Simulation Results

Computer simulations were carried out to evaluate the proposed algorithm's performance in multipath scenarios. To this end, we draw the BER versus the signal-to-noise ratio (SNR) curves. We consider a $(3, 6)$-regular LDPC code of length 4000. The modulation format is B-PAM. In the distributed pilots, one pilot is inserted in every 20 successive symbols, while in the concentrated one a group of 100 pilots is inserted before and after the LDPC Packet. In a baseband communication system, pulse shaping was carried out using a raised cosine filter with a filter span of 10 per symbol, samples of 16 per symbol, i.e., dividing the symbol duration to 16 (16 possible PEs), and the roll-off factor of 0.5. We assumed that the symbol duration is much smaller than the coherent time of the channel; thus, no Doppler effect (otherwise, the baseband pulses will be broadened at the receiver, due to the Doppler effect). We also considered the transmitter and receiver filter delays in our simulations. Attenuation coefficients were randomly chosen from a set of 100 numbers in the range of $[0 : 99] \times \frac{1}{100}$. Please confirm this revision. To simplify the algorithm, we assume that LOS

always exists. The delay profile of the channel follows a Weibull distribution with a scale parameter of 1 and a shape parameter of 0.4. We consider code rate in the computation of noise variance at the receiver. We also set the minimum error packets to 100, detector iterations to 10, maximum number of decoder iterations to 200, and global iterations of the receiver to 5 and 30. We used lookup tables to compute the means of Gaussian likelihoods according to the explained instructions in this paper. Figures 2–5 show the simulation results for the distributed and concentrated pilots. The curve labelled by "LDPC" was obtained through pulse shaping, matched filtering and LDPC decoding in an AWGN channel. The name of the rest of the curves is based on their multipath numbers and global iterations of the receiver, e.g., 3-JDD Glob. It. 5 represents joint detection and decoding in a scenario involving three unknown overlapping paths and 5 overall receiver iterations. The relative solution is obtained through 200 iterations of the decoder and single iteration of the receiver where the observations are computed by $\exp\left\{-\frac{(r_k-c_k)^2}{2\sigma^2}\right\}$. σ^2 is inversely proportional to the average power of the received signal. The relative solution can be used to compare the performance of various algorithms in the multipath scenario. The more an algorithm outperforms the relative solution, the more accurate it is. As the receiver lacks knowledge of the channel parameters, previous methods have been unable to track them, requiring changes to existing algorithms. In response, we present a relative solution that establishes an upper bound for system performance. For simplicity, the simulation assumes that only the number of interfering paths remains fixed at each time epoch.

The results indicate that the performances of distributed and concentrated pilots are nearly identical under the same conditions. In the scenario with two overlapping paths, the proposed algorithm experiences a degradation of 0.6 dB compared with LDPC, and in the scenario with three overlapping paths, this degradation increases to 1 dB. However, in every case, the proposed algorithm outperforms the relative solution by 0.2 dB. Although the difference between 5 and 30 iterations of the receiver is negligible for two overlapping paths, as the number of unknown paths increases, the difference becomes more significant.

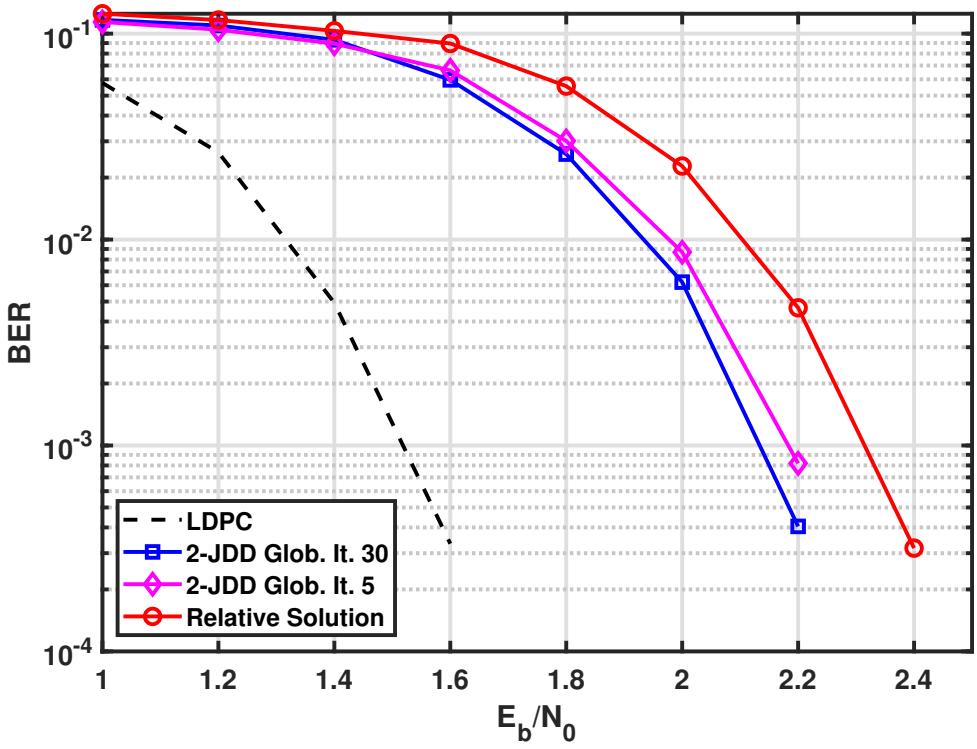

Figure 2. 2-JDD in the distributed pilots, including the lower and upper bounds (LDPC and relative solution).

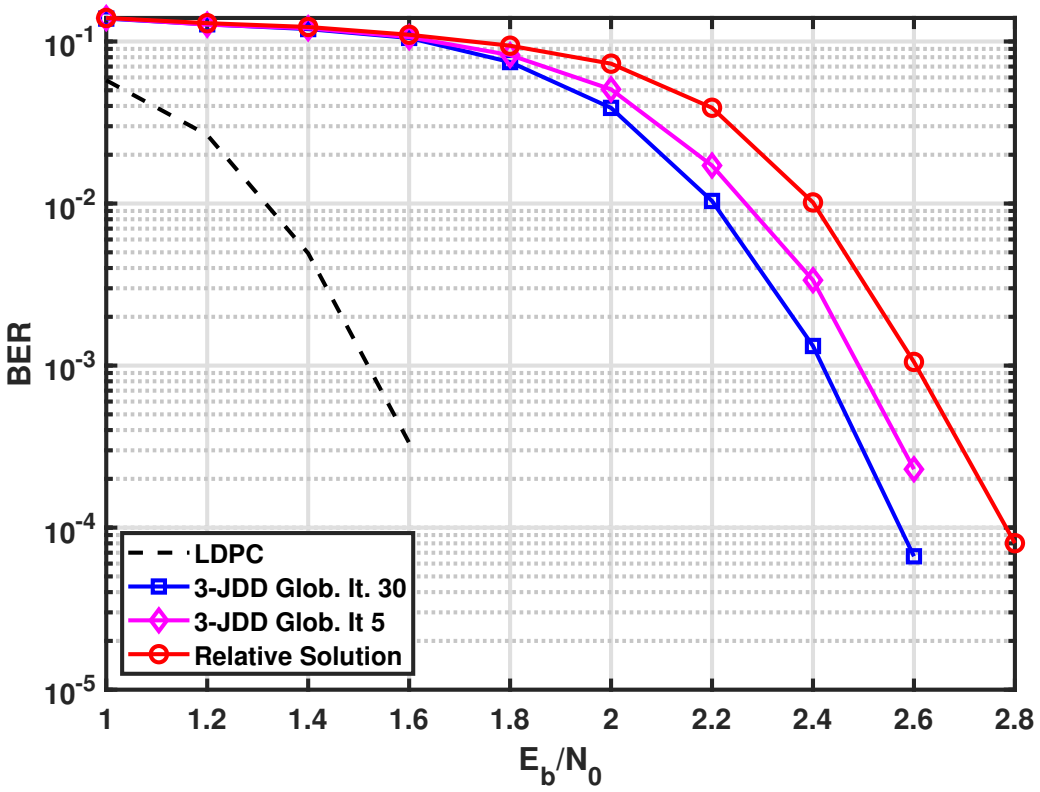

Figure 3. 3-JDD in the distributed pilots pilots, including the lower and upper bounds (LDPC and relative solution).

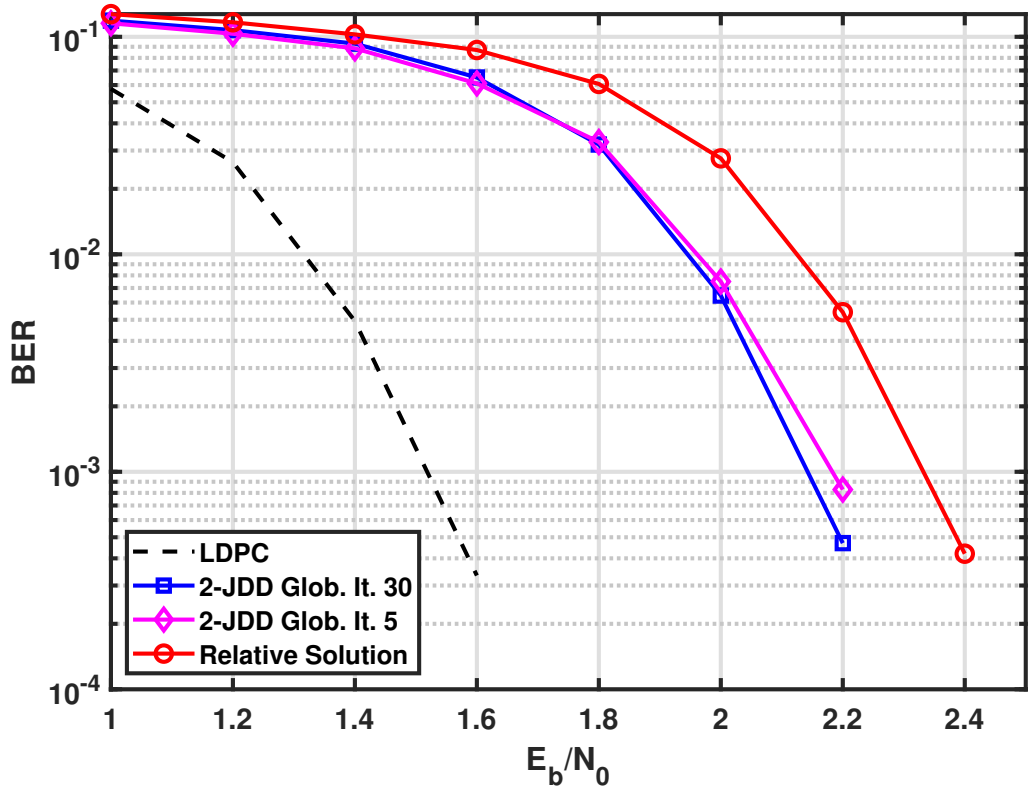

Figure 4. 2-JDD in the concentrated pilots, including the lower and upper bounds (LDPC and relative solution).

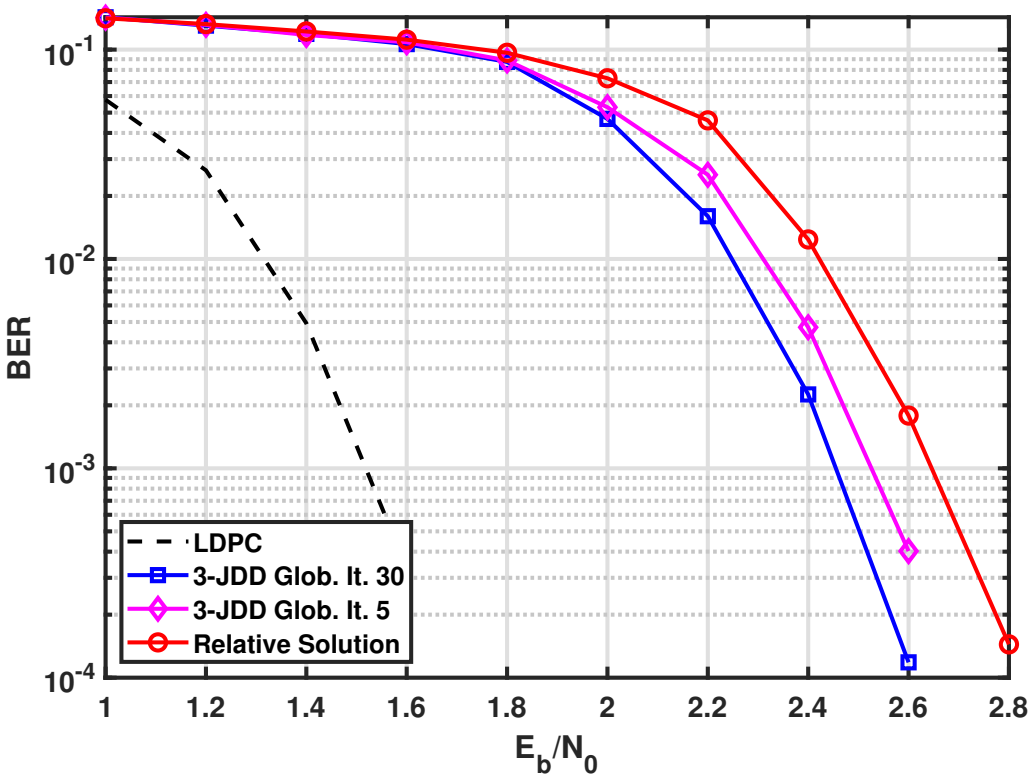

Figure 5. 3-JDD in the concentrated pilots, including the lower and upper bounds (LDPC and relative solution).

We compute the complexity of the proposed algorithms in terms of the number of accesses to the LOTs, the number of operations (additions and multiplications) between two real arguments, and the number of comparisons to find the minimum value of a matrix at each time epoch. The results are summarized in Table 1.

Table 1. Computational Load at each time epoch for B-PAM Modulation.

Operations	LUT Accesses	Comparisons
$(4N^2N' + 8N' + 4)(L-1)$	$6N(L-1)+4$	$\frac{N^2N'}{2} - NN' + N + 2N' - 6$

7. Conclusions and Future Work

In this paper, the tracking of all multipath parameters using SPA was made possible through the front-end consideration of the communication systems. This process was followed by discretizing channel parameters and assigning them Bernoulli random variables. The primary limitation of the algorithm is its complexity in detection of path patterns when the number of interfering paths increases significantly. The use of quantum computing algorithms for path pattern detection could offer a potential solution to this challenge. In future work, we aim to compute the optimal discretization levels.

Author Contributions: Conceptualization, A.M. and A.Z.; methodology, A.M. and A.Z.; software, A.M. and A.Z.; validation, A.M. and A.Z.; formal analysis, A.M. and A.Z.; investigation, A.M. and A.Z.; resources, A.M. and A.Z.; data curation, A.M. and A.Z.; writing—original draft preparation, A.M. and A.Z.; writing—review and editing, A.M. and A.Z.; visualization, A.M. and A.Z.; supervision, A.M. and A.Z.; project administration, A.M. and A.Z. All authors have read and agreed to the published version of the manuscript.

Funding: This research received no external funding.

Institutional Review Board Statement: Not applicable.

Informed Consent Statement: Not applicable.

Data Availability Statement: The original contributions presented in the study are included in the article, further inquiries can be directed to the corresponding author.

Conflicts of Interest: Author Anoush Mirbadin was employed by the SELTA Digital Platforms Company. The remaining authors declare that the research was conducted in the absence of any commercial or financial relationships that could be construed as a potential conflict of interest.

References

1. Pierce, J.N. Theoretical diversity improvement in frequency-shift keying. *Proc. IRE* **1985**, *46*, 903–910. [CrossRef]
2. Brennan, D.G. Linear diversity combining techniques. *Proc. IRE* **1959**, *47*, 1075–1102. [CrossRef]
3. Turin, G.L. On optimal diversity reception. *IRE Trans. Inf. Theory* **1961**, *7*, 154–166. [CrossRef]
4. Kaye, A.; George, D. Transmission of multiplexed PAM signals over multiple channel and diversity systems. *IRE Trans. Commun.* **1970**, *18*, 520–526. [CrossRef]
5. Alamouti, S.M. A simple transmit diversity technique for wireless communications. *IEEE J. Selec. Areas Commun.* **1998**, *16*, 1451–1458. [CrossRef]
6. Prasad, R. *OFDM for Wireless Communications Systems*, 1st ed.; Artech House: London, UK, 2004.
7. Hutter, A.A.; Mekrazi, S.; Getu, B.N.; Platbrood, F. Alamouti-based space-frequency coding for OFDM. *Wirel. Pers. Commun.* **2005**, *35*, 173–185. [CrossRef]
8. Zhang, J.A.; Zhang, F.; Masouros, C.; Heath, R.W.; Feng, Z.; Zheng, L.; Petropulu, A. An overview of signal processing techniques for joint communication and radar sensing. *IEEE J. Sel. Top. Signal Process.* **2021**, *15*, 1295–1315. [CrossRef]
9. Santos, I.; Murillo-Fuentes, J.J.; Arias-de-Reyna, E.; Olmos, P.M. Turbo EP-Based Equalization: A Filter-Type Implementation. *IEEE Trans. Commun.* **2018**, *66*, 4259–4270. [CrossRef]
10. Ahin, S.S.; Cipriano, A.M.; Poulliat, C.; Boucheret, M.L. A Framework for Iterative Frequency Domain EP-Based Receiver Design. *IEEE Trans. Commun.* **2018**, *66*, 6478–6493. [CrossRef]
11. Mirbadin, A.; Vannucci, A.; Colavolpe, G.; Pecori, R.; Veltri, L. Iterative Receiver Design for the Estimation of Gaussian Samples in Impulsive Noise. *Appl. Sci.* **2020**, *11*, 557. [CrossRef]
12. Yang, M.; Bian, C.; Kim, H.S. OFDM-Guided Deep Joint Source Channel Coding for Wireless Multipath Fading Channels. *IEEE Trans. Cog. Commun. Netw.* **2022**, *8*, 584–599.. [CrossRef]
13. Mirbadin, A.; Zaraki, A. Joint Detection and Decoding over Multipath Channels: The Known Path. *TechRxiv* **2023**. [CrossRef]
14. Venus, A.; Leitinger, E.; Tertinek, S.; Meyer, F.; Witrisal, K. Graph-based Simultaneous Localization and Bias Tracking. *IEEE Trans. Wirel. Commun* **2024**, 1. [CrossRef]
15. Proakis, J.G.; Salehi M. *Digital Communications*, 5th ed.; McGraw-Hill Higher Education: New York, NY, USA, 2005.
16. Goldsmith, A. *Wireless Communications*, 1st ed.; Cambridge University Press: New York, NY, USA, 2007.